

PAPER • OPEN ACCESS

An Improved Algorithm for TDOA Trajectory Tracking

To cite this article: Li Beibei *et al* 2019 *IOP Conf. Ser.: Mater. Sci. Eng.* **569** 022033

View the [article online](#) for updates and enhancements.

An Improved Algorithm for TDOA Trajectory Tracking

Li Beibei¹, Hao Zhanjun^{1,2,*}, Dang Xiaochao^{1,2}

¹ College of Computer Science and Engineering, Northwest Normal University, Lanzhou 730070, China.

² Gansu Province Internet of Things Engineering Research Center, Lanzhou 730070, China.

* Correspondence: zhanjunhao@126.com

Abstract: In a precision positioning system, one important source of positioning error is the clock synchronization problem, which is caused by multiple base stations. Therefore, eliminating the clock synchronization problem in a no-line-of-sight (NLOS) environment plays an important role in reducing errors in a positioning system. To address this problem, this study designs a practical experimental environment and proposes the concepts of Time Difference of Arrival (TDOA) and non-line-of-sight-Time Difference of Arrival (N-TDOA). First, the improved TDOA algorithm is used to determine the tag's position; second, the tag's trajectory is drawn at different times; then, a map of the monitored area is loaded, and the tag trajectory is displayed in the actual experimental environment. The experimental results show that the N-TDOA algorithm synchronizes the base stations at the algorithmic layer; thus, deploying network cables or wires to achieve clock synchronization is unnecessary: wireless deployment can be used. In an NLOS environment, the N-TDOA method significantly improves the positioning accuracy compared with that of other algorithms, which facilitates further trajectory tracking research. Overall, the proposed approach improves both the accuracy and stability of trajectory tracking.

1.Introduction

With the continuous improvement of wireless technologies such as Bluetooth, ZigBee and Wi-Fi and the rapid development of ad hoc networks and the Internet of Things, wireless networks have received much attention from academic circles. Moreover, location-based services (LBS) are now generally considered to be a requirement. Less key technologies^[1-4]. The location information helps to provide early warnings^[5], assists in making in-process decisions, and for post-processing of emergencies in the network. Wireless location information has a wide range of applications in both static networks and networks with mobile characteristics^[6], and better location services are based on location technologies^[7]. Therefore, positioning technologies play decisive roles in the further development of wireless networks, and research into positioning technologies is particularly important.

Because the signal propagation environment in indoor positioning is more complicated than that of an outdoor environment, it is difficult to accurately analyse parameters such as signal arrival time or angle of arrival. However, with continuous wireless sensor network (WSN) advancements and developments, academic research is no longer limited to traditional indoor positioning and location sensing techniques. Currently, multiple areas have begun to use radio signals for location sensing. The development of relatively fast and mature location sensing technology is the most prominent for ultra-wide-band (UWB)-based radar systems^[8]. The authors of [9] proposed using the UWB channel based on a human occlusion application scenario proposed. By measuring and analysing TOA ranging error,



Content from this work may be used under the terms of the [Creative Commons Attribution 3.0 licence](https://creativecommons.org/licenses/by/3.0/). Any further distribution of this work must maintain attribution to the author(s) and the title of the work, journal citation and DOI.

this study investigated the influence of human occlusion on TOA ranging error. At present, relatively recent indoor positioning technology based on commercial Wi-Fi equipment has development advantages in all aspects, including indoor intrusion detection, campus security, shopping mall personnel detection, patient monitoring, real-time detection of the elderly and children in homes and other fields.

The 2.4 GHz wireless network band is similar to Bluetooth. The positioning method is also affected by the environment. When an obstacle or electromagnetic waves interfere with the signal, the data will be inaccurate. Compared with the characteristics of other positioning technologies, UWB is a hot topic in the field of RF communication both at home and abroad^[10]. Pulsed UWB (IR-UWB) technology was issued by the US Department of Defence as a UWB technical standard in 1989^[11]. In March 2007, the IEEE released the IEEE802.15.4a-2007 standard based on the UWB physical layer, which was designed to support short-range communications for devices using ultra-low data rates, ultra-low power, and ultra-low complexity in wireless personal area networks. Distance data transmission support^[12]. Compared with other positioning methods, IEEE 802.15.4a UWB has advantages in terms of accuracy, real-time performance and data bandwidth^[13]. The UWB real-time response frequency can reach 10~40 Hz, while other positioning technologies are generally below 1 Hz. IR-UWB has a nanosecond or sub-nanosecond pulse width. Together, the response frequency and pulse width determine the positioning accuracy achievable by UWB, which can reach the centimetre level^[14]. UWB technology has strong multipath resistance, high time resolution and a known penetration capability. These features are beneficial for real-time positioning and dynamic data collection in indoor complex multipath environments^[15].

Current UWB positioning schemes are generally divided into line-of-sight (LOS) and non-line-of-sight (NLOS) environments, and most are based on angle-of-arrival (AOA) estimates. If the base station can perform both TOA and direction-of-arrival (DOA) estimation, only one base station is necessary for positioning. The authors of [16–18] proposed a UWB positioning method based on TOA-DOA joint estimation. In [16], a three-step joint estimation algorithm was proposed. In this algorithm, the TOA (Time-Of-Arrival) estimation is first performed by the threshold correlation method. Then, the least-mean-square algorithm is used to jointly estimate the TOA and the arrival time difference. Finally, the wave is improved. The estimation accuracy of the time difference is obtained by DOA estimation. Another three-step joint estimation algorithm was proposed in [17]. In this approach, the maximum likelihood estimation algorithm is first applied to perform preliminary TOA estimation; then, a further joint estimation of TOA and arrival time difference is conducted. Finally, DOA estimation is carried out using the time difference between the wave time and the geometric triangular cosine theorem. In [18], a two-step joint estimation algorithm was proposed that first uses the TC algorithm to roughly estimate the TOA and then finds the maximum value by a log-likelihood equation. To improve the accuracy of TOA and DOA estimations, the algorithm designed in [16] and [17] requires 3 steps, and the algorithm is more complicated. In contrast, the estimation accuracy of the approach in [18] is limited by the sampling frequency, which is in GHz. Measuring the level using Nyquist frequency entails high system complexity. In [19], a directional differential feed UWB with stable radiation mode was proposed. The antenna design was realized in the NLOS environment to obtain a better signal acquisition performance, but the design method for the LOS environment was not given. The authors of [20] proposed a low-density parity check code for a non-coherent UWB communication system. Two low-density-parity-check codes and their corresponding decoding procedures were proposed for non-coherent UWB systems. In [21], a high-performance compression sampling of an OFDM-UWB system was proposed to solve the UWB signal-sampling problem, but its performance in an NLOS environment does not meet UWB positioning accuracy requirements. In this paper, a large number of experiments are conducted to verify our method's performance. The main contributions and innovations of this paper are as follows:

(1) We establish a UWB trajectory tracking model, perform base-station deployment based on this model, and establish a four-base-station-label UWB trajectory tracking experimental environment.

(2) We propose an improved TDOA algorithm that uses the N-TDOA method to solve the clock synchronization problem introduced by having multiple base stations.

(3) Synchronization is implemented in the algorithm layer using the N-TDOA algorithm, and wireless deployment can be conducted without deploying a network cable or a wire to implement clock synchronization. This reduces signal propagation errors and improves the accuracy of trajectory tracking. On one hand, it reduces the degradation of the signal during NLOS propagation; on the other hand, it eliminates the clock synchronization problem caused by multiple base stations.

(4) We fully verify the performance of the proposed algorithm through experiments conducted in an actual environment. First, the N-TDOA algorithm effectively eliminates the influence of the clock synchronization problem on the positioning accuracy. Second, compared with the existing algorithm, the results show that our algorithm has better performance.

The remaining sections of this article are organized as follows. Section 2 provides an introduction to the related works. Section 3 describes the trajectory tracking method studied in this paper. The experiments presented in Section 4 verify the proposed method. Section 5 summarizes the full text, and Section 6 suggests possible future work.

2. Trajectory Tracking Method

In this section, we mainly introduce the trajectory tracking method.

2.1 Low-Resolution Digital Receiver Architecture

The received UWB multipath signal is expressed as follows:

$$r(t) = \sum_{k=1}^{N_t} d_k \varpi_{mp}(t - kT - \tau_{tot}) + n(t) \quad (1)$$

$$\varpi_{mp}(t) = \sqrt{E_p} \sum_{l=1}^L a_l p(t - \tau_l) \quad (2)$$

where ϖ_{mp} is the received pulse after the channel impulse response, $p(t)$ is a transmission pulse with unit energy considering a second derivative Gaussian single pulse, E_p is the pulse energy, $d_k \in \{-1, 1\}$ is the random polarity code of the k th transmitted symbol, N_t is the symbol number, T is the symbol duration, τ_l and a_l represent the delay of the multipath component and the fading coefficient, respectively, and $n(t)$ represents additive white Gaussian noise (AWGN) with zero mean and variance σ^2 .

The received signal is filtered by a low pass filter (LPF) and then sampled during the sample period (see figure 1). Each symbol is sampled at $N = \lfloor T / T_s \rfloor$ points. The i th full resolution sample of the k th symbol can be written as follows:

$$r_{k,i} = d_k w_i + n_{k,i}, i = 0, 1, \dots, N-1 \quad (3)$$

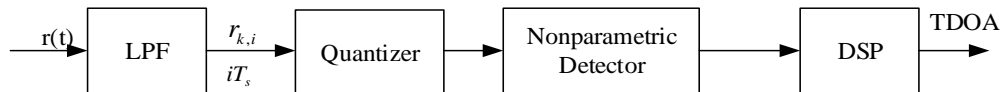


Figure 1. Low-resolution digital receiver architecture.

We collect samples as an observation vector $R = [R_0, R_1, \dots, R_{N-1}]$, where $R_i = [r_{1,i}, r_{2,i}, \dots, r_{N_i,i}]^T$. Then, $r_{k,i}$ is quantified based on carefully designed parameters. Based on the conditional test structure, a test statistic is generated in the non-parametric detector that adds noise under the assumption of the symmetric density function to present a constant false alarm probability. Finally, the digital signal processing (DSP) portion of the receiver provides the final TDOA results.

2.2 Improve the Principle of TDOA Positioning

The standard TDOA algorithm involves transmitting a UWB pulse signal when the four base stations are completely synchronized; then, the tag is positioned by the arrival time difference of the UWB signal sent by each base station and by combining the position coordinates of the base station. As shown in figure 2, the signals of the respective base stations go through various complicated channels in the process of reaching the tag: the channels are multipath and have NLOS errors, so the time when the signals arrive at the tags from the base station is often much larger than the signal pulse time of one base station. If the guard time slot is not added, the signal of a previous base station can collide with a later one, causing the label to be unable to distinguish the base station.

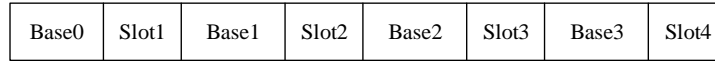


Figure 2. Base station access under standard TDOA.

The TDOA algorithm can make a set of hyperbolae by comparing the arrival time difference of the signal. As shown in figure 3(a), the intersection of the hyperbola is the position of the tag, and the focus of each hyperbola is the position of the base station.

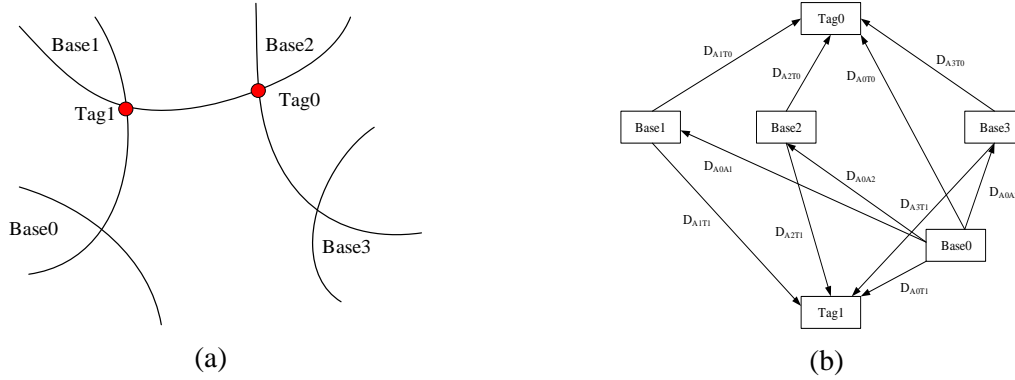


Figure 3. Positioning network model of the TDOA algorithm. (a) Standard TDOA. (b) Improved TDOA.

The TDOA equation obtained based on the time difference of arrival is:

$$\begin{cases} \sqrt{(x-x_2)^2 + (y-y_2)^2} - \sqrt{(x-x_1)^2 + (y-y_1)^2} = c \cdot (t_2 - t_1) \\ \sqrt{(x-x_3)^2 + (y-y_3)^2} - \sqrt{(x-x_1)^2 + (y-y_1)^2} = c \cdot (t_3 - t_1) \\ \vdots \\ \sqrt{(x-x_n)^2 + (y-y_n)^2} - \sqrt{(x-x_1)^2 + (y-y_1)^2} = c \cdot (t_n - t_1) \end{cases} \quad (4)$$

where: (x_n, y_n) is the coordinates of the base station; (x, y) is the coordinates of the tag, t_n is the time at which the n th base station arrives at the tag, and c is the velocity of the electromagnetic wave, 3×10^8 m/s. The TDOA standard algorithm can derive the label coordinates from equation (4). The TDOA standard algorithm requires clock synchronization between the base stations, base station signalling, and tag reception. Due to the complete synchronization of the base stations, the optimal solution can be obtained mathematically, for example, by the least squares method, linear constraint, and the like. The tag calculates its position based on the arrival time difference, the guard time slot, and the coordinates of the base station.

However, the high requirements for the complete synchronization of the base station of the TDOA standard algorithm can fail due to the inaccuracy of the crystal frequency, the influence of the ambient temperature, etc., causing the base station to be incompletely synchronized at the initial time. In addition, even if the clock synchronization of the initial state is realized because the frequencies of the crystal oscillators differ slightly, clock drift will occur over time, and the base stations will become desynchronized. The traditional approach to TDOA synchronization uses network cables or other

wires to avoid desynchronization, but it has limitations, which is easily limited by geographical factors, cannot be deployed on a large scale, and cannot achieve wireless clock synchronization. Moreover, it is difficult to deploy and cannot be applied commercially. To solve this problem, the improved TDOA algorithm is used to realize wireless clock synchronization.

The improved TDOA algorithm differs from the standard TDOA algorithm in that the base stations can achieve initial clock synchronization more easily and more conveniently than with the standard algorithms. Thus, the new algorithm further reduces the difficulty of clock synchronization and is easy to implement wirelessly.

As shown in figure 3(b), $DA_0T_0, DA_1T_0, DA_2T_0, DA_3T_0$ are the distances between the four base stations and tag0, and DA_0A_1, DA_0A_2 and DA_0A_3 are the distances between base station0 and the other base stations. Base station0 sends a signal to the entire network, and the other base stations transmit a signal to tag0 as soon as they receive the signal from base station0. Upon receiving the signal from base station0, tag0 records the arrival time of the signal and then waits until the signals from the base station1, the base station2, and the base station3 have arrived. Then, tag0 records the arrival time t_0 from all the base stations to the and calculates the arrival time differences $(t_1 - t_0), (t_2 - t_0), \dots, (t_n - t_0)$ between base station1, base station2, base station3, ..., base station n. It calculates its own coordinates by combining their coordinates. Because tag0 records the arrival times of base station0 using a local clock, in the new algorithm, this is equivalent to the same signal starting from a randomly selected base station0 and passing through different paths to tag0, and their starting times are essentially consistent, which achieves the initial clock synchronization of the base stations. The TDOA improved algorithm achieves synchronization at the algorithm layer; consequently, there is no need to deploy network cables or wires to achieve clock synchronization, and the scheme can be deployed wirelessly. Therefore, the improved TDOA algorithm is useful for indoor positioning. Figure 3(b) shows a location network model of the improved TDOA algorithm.

The TDOA improvement algorithm applies the following equations:

$$\begin{cases} D_{A_0A_1} + \hat{D}_{A_1T_0} - \hat{D}_{A_0T_0} = c \bullet (t_2 - t_1) \\ D_{A_0A_2} + \hat{D}_{A_2T_0} - \hat{D}_{A_0T_0} = c \bullet (t_3 - t_1) \\ \vdots \\ D_{A_nA_3} + \hat{D}_{A_nT_0} - \hat{D}_{A_0T_0} = c \bullet (t_n - t_1) \end{cases} \quad (5)$$

where t_n is the time at which base station n arrives at tag0, $\hat{D}_{A_nT_0} = \sqrt{(\hat{x} - x_n)^2 + (\hat{y} - y_n)^2}$; (\hat{x}, \hat{y}) are the estimated coordinates of tag0, (x_n, y_n) are the coordinates of base station n, and $\hat{D}_{A_nT_0}$ is the moment estimate of the distance between the base station and the tag. Because the distance between base station0 and base station n can be measured by the field, no moment estimate is needed. In the TDOA positioning process, the tag receives signals, but it does not send signals; therefore, it does not generate collision interference. Tag0 and tag1 are relatively independent so that multi-tag extension can be realized. Thus, the improved TDOA algorithm achieves clock synchronization of the base stations.

2.3 Positioning Trajectory Tracking Model

The trajectory tracking model of this paper is determined by the N-TDOA algorithm. The trajectory tracking framework is shown in figure 4:

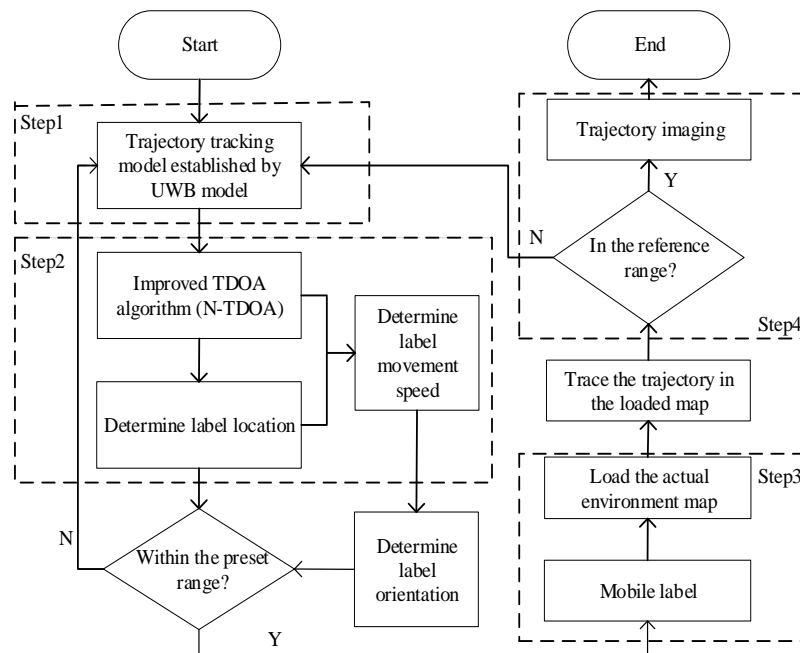


Figure 4. Trajectory tracking model.

Through the above framework diagram, the trajectory tracking method of this paper is divided into the following four steps:

Step1: Determine the trajectory tracking framework by UWB positioning principle;

Step 2: Estimate the tag location using the improved TDOA algorithm N-TDOA. Specifically, the label direction is determined by determining the label moving speed, and if the calculation result continues in step 3 in the preset range, otherwise returns to step 1;

Step3: Move the label and load the actual environment map;

Step4: Track the trajectory in the loaded actual map. If the tracking result is within the set range, the trajectory tracking result is output, otherwise it returns to step1.

3. Lab Environment

3.1 Actual Experimental Environment

In this paper, the experimental environment is full of obstacles in the laboratory, conference rooms and empty corridors, the size is set to 3m*3m, in order to verify the signal transmission law of the algorithm and the performance of the N-WLS algorithm in the complex environment. The actual environment diagram is shown in figure 5, and the environment plan is shown in figure 6. We select the experimental platform is the I-UWB LPS positioning system. Based on the debugging terminal of INFAssistant serial port provided by Infinity Future website, this paper improves INFAssistant 1.01, to realize real-time updating of motion track, loading of map in experimental environment, displaying of signal waveform in two and three dimensions, debugging of serial port and so on. It provides a more intuitive form of expression for trajectory tracking. At the same time, through the improvement of our team, the system has achieved the estimation and tracking accuracy of a single tag 5cm.

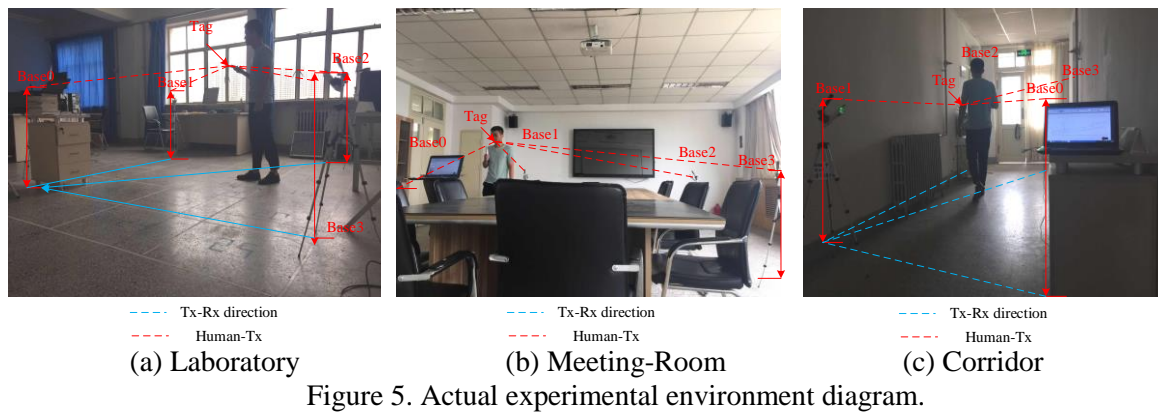


Figure 5. Actual experimental environment diagram.

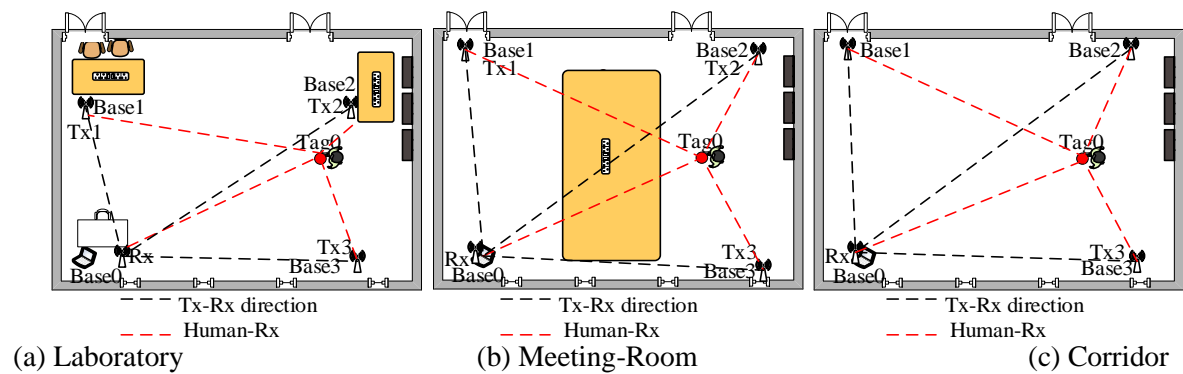


Figure 6. Diagram of the experimental environment.

3.2 Hardware Test Environment

The hardware used in this study was the I-UWB LPS positioning system. This study improves INFAssistant 1.01 based on the INFAssistant serial debugging terminal provided by the Infinite Future official website, to realize real-time updating of a motion trajectory, loading of the experimental environment map, 2D and 3D displays of the signal waveforms, serial port debugging and other functions. These features provide a more intuitive representation of trajectory tracking. At the same time, the system achieves an estimated tracking accuracy of 5 cm for a single tag. The specific hardware test environment is shown in Figure 7. Figure 6(a) shows a positioning module of the base station and the tag; (b) shows a power module; (c) shows a networking diagram of the nodes.

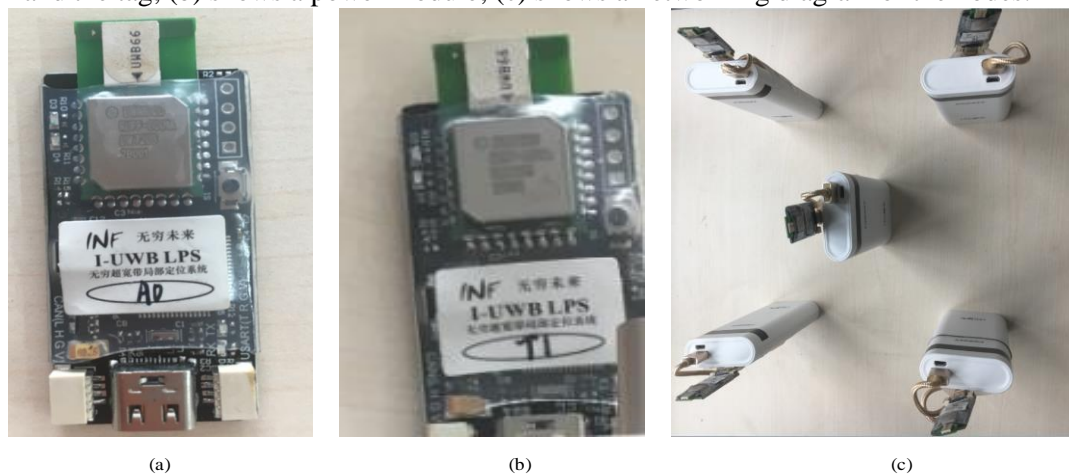


Figure 7. Hardware testbed; (a) Base station; (b) Power supply; (c) Network diagram.

4. Analysis of Experimental Results

4.1 Test Results

The experiments were divided into three groups to observe the changes in the x and y-axis signals, respectively, and the z-axis signal changes in three dimensions. The first group of testers walked at a constant speed of 1 m/s within the set's 3 m*3 m area, as shown in figure 8.

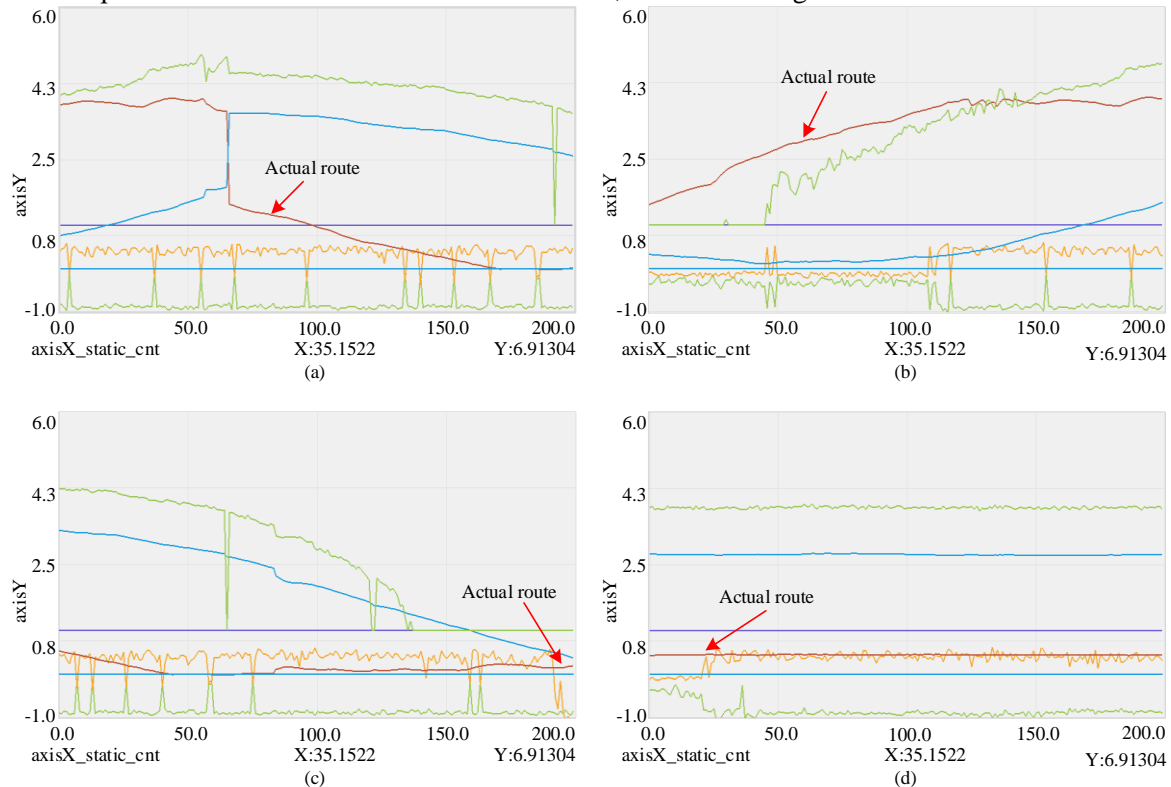


Figure 8. Walking at a constant speed of 1 m/s.

The experimental results show that the signal changes in the x, y, and z-axes are slight when a tester is walking at a speed of 1 m/s, as shown in figure 8(a)-8(c). The signal changes in the selected three different positions of the testers, and the signal fluctuations continue to be stable. In particular, the z-axis signal is shown in figure 8(d). The signal remains essentially the same when the tester is walking at a constant speed. Because the tester was moving along the edge of the set area during the experiment, the influence of the distance between the tag and the base station is basically eliminated, further indicating that the signal fluctuations are related to the speed and uniformity of the tester's motion.

The second group of testers moved along a z-shaped uniform motion trajectory at a speed of 1 m/s within the set area, as shown in figure 9.

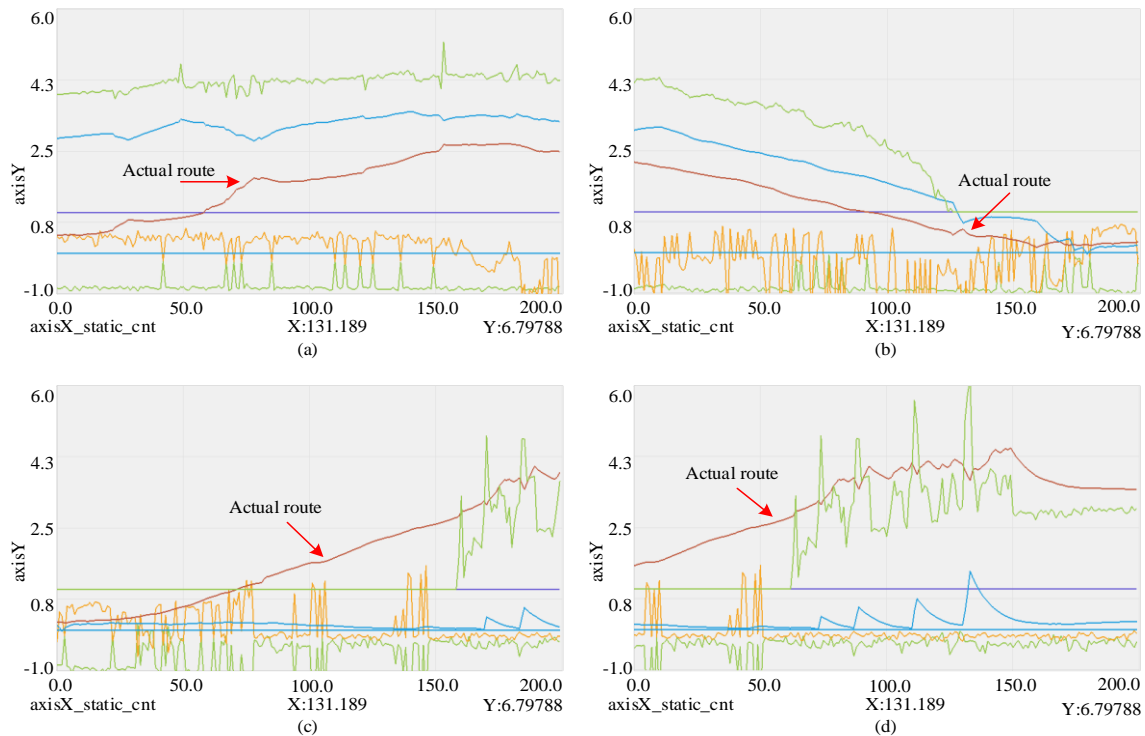


Figure 9. Z-shaped track walking at a constant speed of 1 m/s.

In figure 8, the signal changes in the x, y, and z-axes as the tester walks a z-shaped pattern within the test area can be seen. Figure 9(a) and 9(c) show the change in the z-axis, which is basically stable because the tester's movement amplitude is relatively small, which basically excludes the influence of the tester's height. However, the changes in the x- and y-axis signals during the motion, as shown in figure 9(b) and 9(d), show that the fluctuations are uniform and obvious. The influence of height and the uniform velocity can be explained by the signal fluctuations and the tester's distance from the base station tag.

The results of the third group of testers, who walked at non-uniform speeds of approximately 1 m/s are shown in figure 10. Through these three experiments, we were able to analyse the relationships between UWB signal fluctuation and personnel height, walking speed, base station and tag distance. This analysis provides more precise supporting principles for achieving accurate human motion trajectories.

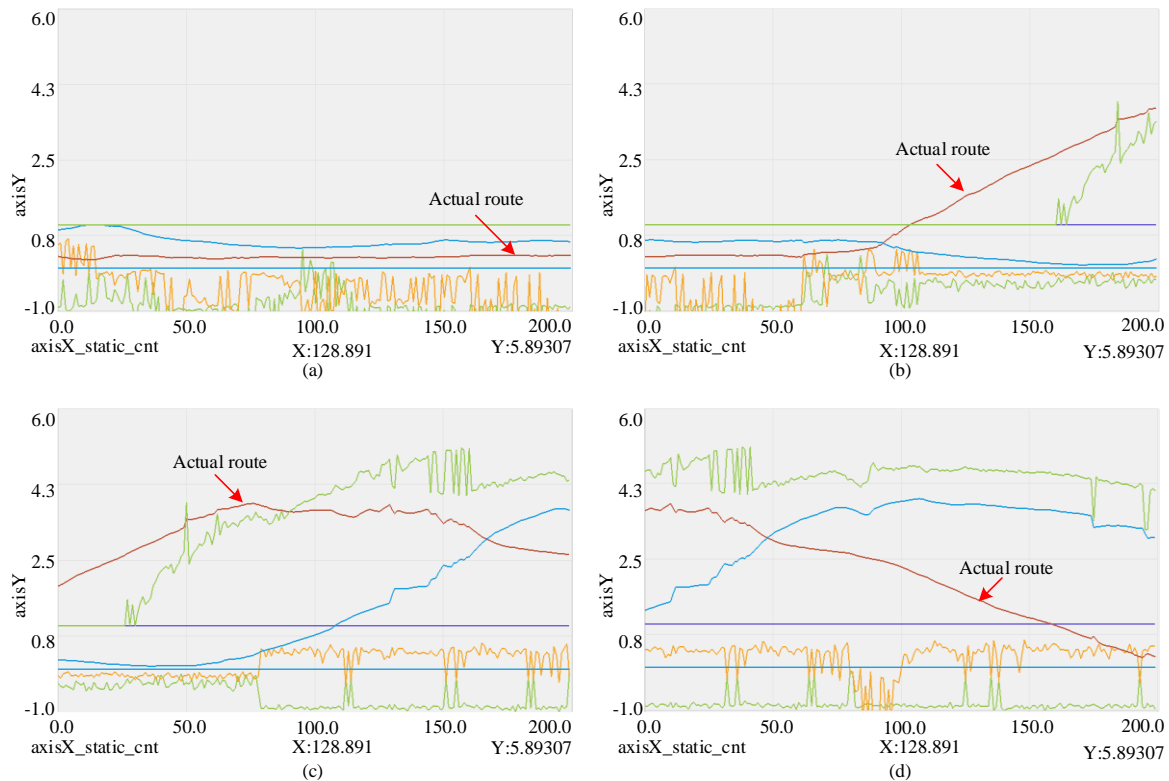


Figure 10. Non-uniform walking at 1 m/s.

Figure 10 shows the signal changes of the x, y, and z-axes when the tester moves at a non-uniform speed of 1 m/s within the test area. The signal fluctuations are relatively obvious. A comparison with figures 8 and 9 further illustrates that the signal fluctuations are related to the distance between the base station tag and the tester's speed.

4.2 Trajectory Tracking Results

The trajectory tracking results of the three groups of experimental testers in this paper are shown in figure 11. The first group of testers walked at a constant speed of 1 m/s within a $3\text{ m} \times 3\text{ m}$ area, as shown in figure 11(a) and 11(d). The second group is the result of the tester moving along a z-shaped uniform motion trajectory at a speed of 1 m/s within the set area, as shown in figure 11(b) and 11(e). The third group of testers walked at non-uniform speeds of 1 m/s, as shown in figure 11(c) and 11(f). The trajectory tracking results were displayed on the host computer. Because the display was in real-time, the trajectory tracking results cannot be fully displayed in a static image. However, a comparison between the actual trajectory and the simulated trajectory can be obtained. The method has good trajectory tracking results in all three groups of experiments.

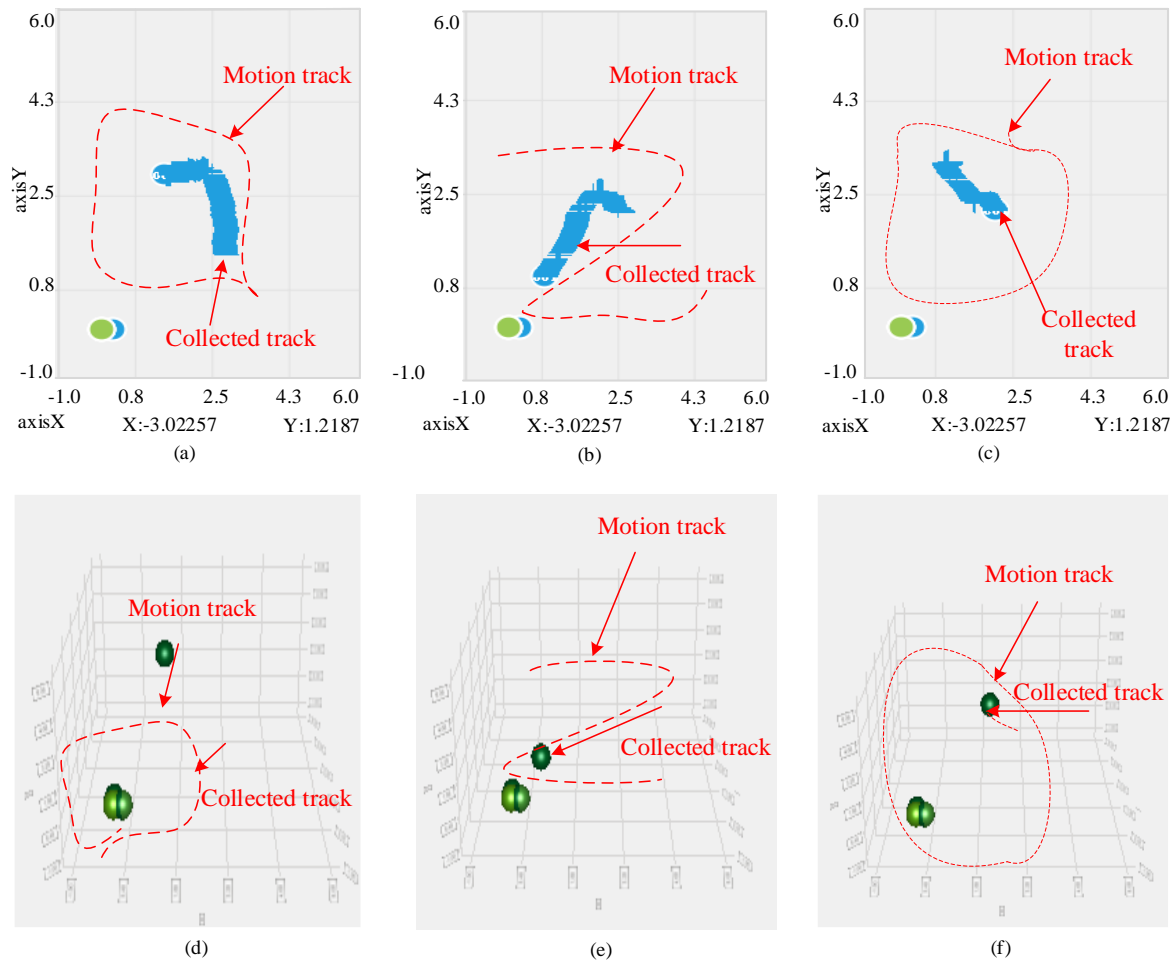


Figure 11. Trajectory tracking results of three sets of experiments.(a) Walking at a constant speed of 1 m/s;(b) Z-shaped track walking at 1 m/s;(c) Non-uniform walking at 1 m/s;(d) The result of walking at a constant speed of 1 m/s;(e) The result of z-shaped track walking at 1 m/s;(f) The result of non-uniform walking at 1 m/s.

As shown in figure 11, (a), (b), and (c) respectively represent actual running trajectories of people at different speeds and different motion states, and corresponding (d), (e), and (f) respectively represent three-dimensional space. The movement of the person in the middle, the figure can clearly know that the speed and the movement mode have a great influence on the result of the trajectory tracking, especially when the person has zigzag movement, the effect of the trajectory tracking is more obvious. The superior performance of the algorithm in trajectory tracking is further illustrated.

4.3 Performance Comparison Analysis

To further demonstrate the performance of the improved N-TDOA method, we compare it with the currently used TOA algorithm, the Chan algorithm and the K-means algorithm using the same three groups of experiments described above. The results are shown in figure 12.

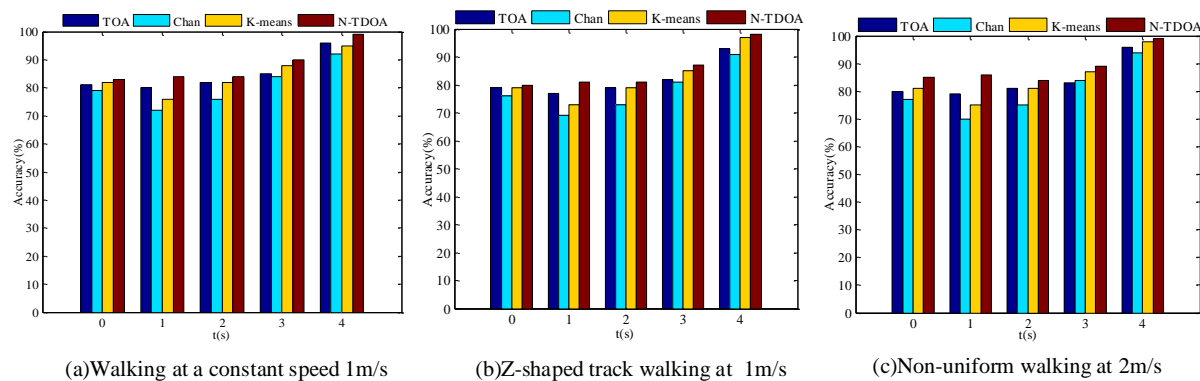


Figure 12. Accuracy comparison of four methods under three sets of experiments.

As figure 12 shows, these three experiments, the N-TDOA method proposed in this paper performs better than does the other three methods, especially in the third group of experiments; its improved accuracy is obvious. These results occur because as the testers' motion speeds, distances from a base station label, heights, and walking speeds vary, the other three algorithms cannot eliminate each other's influences, while the proposed algorithm is well suited to the signal. Separation is performed to keep the signal clock steady to achieve a more stable performance. The trajectory tracking results obtained from the above three sets of experiments illustrate the effectiveness and stability of this method.

5. Conclusions

Based on the advantages of previous positioning methods, this paper proposes using the local positioning system II-UWB LPS to eliminate the clock synchronization problem caused by multiple base stations in environments with four base stations and one tag. The improved TDOA algorithm determines the position of a tag and the positions of pre-determined tags at different times to acquire the tag trajectory. Then, it loads a map of the monitored area and displays the tag trajectory in the actual experimental environment. The experimental results show that the N-TDOA algorithm is synchronized at the algorithmic layer; therefore, deploying network cables or wires to achieve clock synchronization is unnecessary: wireless deployment can be used instead. The trajectory tracking accuracy of the N-TDOA method in the NLOS environment is significantly improved compared with that of other algorithms. Therefore, in the future work, multi-person trajectory tracking will be the focus of research.

Authors' contributions

BBL contributed to algorithm creation and to the analysis. As the supervisor of ZJH, he proofread the paper several times and provided guidance throughout the entire manuscript preparation process. XCD contributed to the algorithms, the analysis, and the simulations and wrote the paper. BBL and ZJH revised the equations, helped write the introduction and related works sections, and critically revised the paper. All the authors have read and approved the final manuscript.

Data Availability

This experiment was obtained in a real experimental environment, all data is actually available, and the relevant data has been described in the article. I am happy to share all the data in the article, because all the data in this article is obtained through the real experimental environment, so I don't use any other people's support data, it means no data were used to support this study.

Conflicts of Interest

The authors declare that there is no conflict of interest regarding the publication of this paper.

Funding Statement

This work was supported by the National Natural Science Foundation of China under Grant No. 61762079 and No. 61662070; the Key Science and Technology Support Programme of Gansu Province under Grant No. 1604FKCA097 and No. 17YF1GA015; and the Science and Technology Innovation Project of Gansu Province under Grant No. 17CX2JA037 and No. 17CX2JA039.

Acknowledgements

The authors would like to thank the reviewers for their thorough reviews and helpful suggestions.

References

- [1] Z. Qian, D. Sun, and V. Leung, "Overview of wireless network positioning," *Chinese Journal of Computers*, vol. 39, no. 6, pp. 1237–1256, 2016.
- [2] Y. Liu, Z. Yang, X. Wang, and L. Jian, "Location, localization, and localizability," *Journal of Computer Science and Technology*, vol. 25, no. 2, pp. 274–297, 2010.
- [3] Y. Gu, Y. Chen, J. Liu, and X. Jiang, "Semi-supervised deep extreme learning machine for Wi-Fi based localization," *Neurocomputing*, vol. 166, pp. 282–293, 2015.
- [4] C. Tsirmpas, A. Rompas, O. Fokou, and D. Koutsouris, "An indoor navigation system for visually impaired and elderly people based on Radio Frequency Identification (RFID)," *Information Sciences*, vol. 320, pp. 288–305, 2015.
- [5] Y. Ji, "Navigation using environmental constraints," in *6th IEEE Consumer Communications and Networking Conference*, pp. 1–5, IEEE, Las Vegas, NV, USA, 2009.
- [6] I. Amundson and X. D. Koutsoukos, "A survey on localization for mobile wireless sensor networks," in *International Conference on Mobile Entity Localization and Tracking in Gps-Less Environments*, pp. 235–254, Springer, Berlin, Heidelberg, 2009.
- [7] P. Q. Jin, W. Na, X. X. Zhang, and L. Yue, "Moving object data management for indoor spaces," *Chinese Journal of Computers*, vol. 38, no. 9, pp. 1777–1795, 2015.
- [8] Y. Zhang, Jinsen Y U, Hao P, et al. Node Localization of Wireless Sensor Network Based on Weighted Evaluation Mechanism of Linear Parameter[J]. *Computer Engineering*, 2017.
- [9] Jie H E, Ya-Nan W U, Duan S H, et al. Model of human body influence on UWB ranging error[J]. *Journal on Communications*, 2017.
- [10] Q. Zhou, C. Wu, J. Xing et al., "Wi-dog: monitoring school violence with commodity wifi devices," in *Wireless Algorithms, Systems, and Applications*, pp. 47–59, Springer International Publishing, Cham, 2017.
- [11] X. Ding, Q. Wang. Wi-Fi indoor localization algorithm based on improved support vector machine[J]. *Computer Engineering & Applications*, 2016.
- [12] W. Zhang T, He-Wu L I, Center I T, et al. Indoor WLAN Positioning and Tracking Scheme Based on Signal Propagation Characteristic[J]. *Journal of Chinese Computer Systems*, 2014, 35(7):1447-1452.
- [13] D. Qingxi. Research on Pedestrian Movement Track Recognition Based on Machine Vision[D]. Xi'an University of Technology, 2015.
- [14] L. Gong, W. Yang, Z. Zhou et al., "An adaptive wireless passive human detection via fine-grained physical layer information," *Ad Hoc Networks*, vol. 38, pp. 38–50, 2016.
- [15] R. Zhou, X. Lu, P. Zhao, and J. Chen, "Device-free presence detection and localization with SVM and CSI fingerprinting," *IEEE Sensors Journal*, vol. 17, no. 23, pp. 7990–7999, 2017.
- [16] J. Wang, H. Jiang, J. Xiong et al., "LiFS: low human-effort, device-free localization with fine-grained subcarrier information," in *International Conference on Mobile Computing and Networking*, pp. 243–256, ACM, New York, NY, 2016.
- [17] Y. Xie, Z. Li, and M. Li, "Precise power delay profiling with commodity wifi," in *International Conference on Mobile Computing and Networking*, pp. 53–64, ACM Press, New York, NY, 2015.

- [18] J. Li, Y. Li, and X. Ji, "A novel method of Wi-Fi indoor localization based on channel state information," in 8th International Conference on Wireless Communications & Signal Processing (WCSP), pp. 1–5, IEEE, Yangzhou, China, 2016.
- [19] Y. Fang, B. Wang, C. Sun, Z. Song, and S. Wang, "A directional differential-fed UWB antenna with stable radiation pattern," *Journal of Nanjing University of Aeronautics and Astronautics*, vol. 33, no. 6, pp. 747–753, 2016.
- [20] Z. Liang, J. Zang, X. Yang, X. Dong, and H. Song, "Low-density parity-check codes for noncoherent UWB communication systems," *China Communications*, vol. 14, no. 7, pp. 1–11, 2017.
- [21] L. Ge, H. Zhang, H. Guo, and H. Wu, "High performance compressed sampling for OFDM-UWB systems," *China Communications*, vol. 14, no. 3, pp. 75–86, 2017.